

# A light pseudoscalar of 2HDM confronted with muon g-2 and experimental constraints

Lei Wang, Xiao-Fang Han

*Department of Physics, Yantai University, Yantai 264005, PR China*

## Abstract

A light pseudoscalar of the lepton-specific 2HDM can enhance the muon g-2, but suffer from various constraints easily, such as the 125.5 GeV Higgs signals, non-observation of additional Higgs at the collider and even  $B_s \rightarrow \mu^+ \mu^-$ . In this paper, we take the light CP-even Higgs as the 125.5 GeV Higgs, and examine the implications of those observables on a pseudoscalar with the mass below the half of 125.5 GeV. Also the other relevant theoretical and experimental constraints are considered. We find that the pseudoscalar can be allowed to be as low as 10 GeV, but the corresponding  $\tan \beta$ ,  $\sin(\beta - \alpha)$  and the mass of charged Higgs are strongly constrained. In addition, the surviving samples favor the wrong-sign Yukawa coupling region, namely that the 125.5 GeV Higgs couplings to leptons have opposite sign to the couplings to gauge bosons and quarks.

PACS numbers: 12.60.Fr, 14.80.Ec, 14.80.Bn

## I. INTRODUCTION

The ATLAS and CMS Collaborations found a 125.5 GeV Higgs boson at the LHC [1, 2]. The latest experimental data show that the properties of this particle agree with the Standard Model (SM) predictions. Especially the diphoton signal strength is changed from  $1.6 \pm 0.4$  to  $1.17 \pm 0.27$  for ATLAS [3] and from  $0.78_{-0.16}^{+0.28}$  to  $1.12_{-0.32}^{+0.37}$  for CMS [4], which are well consistent with the SM prediction within  $1\sigma$  range. Thus, the 125.5 GeV Higgs signal data can give the strong constraints on the effects of new physics.

The two-Higgs-doublet model (2HDM) has very rich Higgs phenomenology, including two neutral CP-even Higgs bosons  $h$  and  $H$ , one neutral pseudoscalar  $A$ , and two charged Higgs  $H^\pm$ . The recent Higgs data have been used to constrain the 2HDM, see some recent examples [5]. In addition, a light pseudoscalar with a large  $\tan\beta$  can account for the  $3.1\sigma$  deviation between the SM predicted and measured values of the muon anomalous magnetic moment [6–9]. Due to the experimental constraints, the type-II 2HDM [10] is very difficult to explain the muon  $g-2$  anomaly [7, 9], but the lepton-specific 2HDM (L2HDM) [11] can still give a valid explanation [8, 9]. Compared to the recent study [9], we focus on a light pseudoscalar for which a relative small  $\tan\beta$  is required to account for the muon  $g-2$  anomaly. For a light pseudoscalar, the 125.5 GeV Higgs decay into the pseudoscalars is open, and the rare decay  $B_s \rightarrow \mu^+\mu^-$  can obtain the additional important contributions from the very light pseudoscalar exchange diagrams. Therefore, the 125.5 GeV Higgs signal data and even  $B_s \rightarrow \mu^+\mu^-$  can give the important constraints on the very light pseudoscalar. Also we consider the theoretical constraints, electroweak precision data, the non-observation of additional Higgs at collider, and the flavor observables  $B \rightarrow X_s\gamma$ ,  $\Delta m_{B_s}$  and  $\Delta m_{B_d}$ .

Our work is organized as follows. In Sec. II we recapitulate the L2HDM. In Sec. III we introduce the numerical calculations. In Sec. IV, we show the implications of muon  $g-2$  and experimental data on the L2HDM. Finally, we give our conclusion in Sec. V.

## II. L2HDM

The general Higgs potential is written as [12]

$$\begin{aligned}
V = & m_{11}^2(\Phi_1^\dagger\Phi_1) + m_{22}^2(\Phi_2^\dagger\Phi_2) - \left[ m_{12}^2(\Phi_1^\dagger\Phi_2 + \text{h.c.}) \right] \\
& + \frac{\lambda_1}{2}(\Phi_1^\dagger\Phi_1)^2 + \frac{\lambda_2}{2}(\Phi_2^\dagger\Phi_2)^2 + \lambda_3(\Phi_1^\dagger\Phi_1)(\Phi_2^\dagger\Phi_2) + \lambda_4(\Phi_1^\dagger\Phi_2)(\Phi_2^\dagger\Phi_1) \\
& + \left[ \frac{\lambda_5}{2}(\Phi_1^\dagger\Phi_2)^2 + \text{h.c.} \right] + \left[ \lambda_6(\Phi_1^\dagger\Phi_1)(\Phi_1^\dagger\Phi_2) + \text{h.c.} \right] \\
& + \left[ \lambda_7(\Phi_2^\dagger\Phi_2)(\Phi_1^\dagger\Phi_2) + \text{h.c.} \right]. \tag{1}
\end{aligned}$$

In this paper we focus on the CP-conserving case where all  $\lambda_i$  and  $m_{12}^2$  are real. In the L2HDM, a discrete  $Z_2$  symmetry is introduced to make  $\lambda_6 = \lambda_7 = 0$ , and allow for a soft-breaking term with  $m_{12}^2 \neq 0$ . The two complex scalar doublets have the hypercharge  $Y = 1$ ,

$$\Phi_1 = \begin{pmatrix} \phi_1^+ \\ \frac{1}{\sqrt{2}}(v_1 + \phi_1^0 + ia_1) \end{pmatrix}, \quad \Phi_2 = \begin{pmatrix} \phi_2^+ \\ \frac{1}{\sqrt{2}}(v_2 + \phi_2^0 + ia_2) \end{pmatrix}. \tag{2}$$

Where the vacuum expectation values (VEVs)  $v^2 = v_1^2 + v_2^2 = (246 \text{ GeV})^2$ , and the ratio of the two VEVs is defined as usual to be  $\tan\beta = v_2/v_1$ . There are five mass eigenstates: two neutral CP-even  $h$  and  $H$ , one neutral pseudoscalar  $A$ , and two charged scalar  $H^\pm$ . We can rotate this basis to the Higgs basis by a mixing angle  $\beta$ , where the VEV of  $\Phi_2$  field is zero. In the Higgs basis, the mass eigenstates are obtained from

$$\begin{aligned}
h &= \sin(\beta - \alpha)\phi_1^0 + \cos(\beta - \alpha)\phi_2^0, \\
H &= \cos(\beta - \alpha)\phi_1^0 - \sin(\beta - \alpha)\phi_2^0, \\
A &= a_2, \quad H^\pm = \phi_2^\pm. \tag{3}
\end{aligned}$$

The right fields of the equations denote the interaction eigenstates in the Higgs basis. The corresponding masses and couplings of Eq. (1) are changed in the Higgs basis [13]. For example, both  $\lambda_6$  and  $\lambda_7$  are taken as zero in the physics basis, but the rotation into the Higgs basis can generate non-zero values for  $\lambda_6$  and  $\lambda_7$ .

In the Higgs basis, the general Yukawa interactions with no tree-level FCNC are give [14]

$$\mathcal{L}_Y = -\frac{\sqrt{2}}{v} \left[ M'_d \bar{Q}_L(\Phi_1 + \kappa_d \Phi_2) d_R + M'_u \bar{Q}_L(\tilde{\Phi}_1 + \kappa_u \tilde{\Phi}_2) u_R + M'_\ell \bar{L}_L(\Phi_1 + \kappa_\ell \Phi_2) \ell_R \right] + \text{h.c.}, \tag{4}$$

where  $\tilde{\Phi}_i(x) = i\tau_2 \Phi_i^*(x)$  and  $M'_{d,u,\ell}$  are the Yukawa matrices. For the L2HDM,

$$\kappa_u = \kappa_d = \cot\beta, \quad \kappa_\ell = -\tan\beta. \tag{5}$$

The couplings of neutral Higgs bosons with respect to the SM Higgs boson are give by

$$\begin{aligned}
y_V^h &= \sin(\beta - \alpha), & y_f^h &= \sin(\beta - \alpha) + \cos(\beta - \alpha)\kappa_f, \\
y_V^H &= \cos(\beta - \alpha), & y_f^H &= \cos(\beta - \alpha) - \sin(\beta - \alpha)\kappa_f, \\
y_V^A &= 0, & y_u^A &= -i\gamma^5\kappa_u, & y_{d,\ell}^A &= i\gamma^5\kappa_{d,\ell}.
\end{aligned} \tag{6}$$

Where  $V$  denotes  $Z$  and  $W$ , and  $f$  denotes  $u$ ,  $d$  and  $\ell$ . The charged Higgs couplings are give as

$$\mathcal{L}_Y = -\frac{\sqrt{2}}{v} H^+ \left\{ \bar{u} [\kappa_d V_{CKM} M_d P_R - \kappa_u M_u V_{CKM} P_L] d + \varsigma_\ell \bar{\nu} M_\ell P_R \ell \right\} + h.c., \tag{7}$$

where  $M_f$  are the diagonal fermion mass matrices.

### III. NUMERICAL CALCULATIONS

The in-house code is used to calculate the muon g-2,  $\chi^2$  fit to 125.5 GeV Higgs signal,  $B_s \rightarrow \mu^+ \mu^-$ ,  $\Delta m_{B_s}$  and  $\Delta m_{B_d}$ . 2HDMC-1.6.5 [15] is employed to implement the theoretical constraints from the vacuum stability, unitarity and coupling-constant perturbativity, and calculate the oblique parameters ( $S$ ,  $T$ ,  $U$ ) and  $\delta\rho$ . SuperIso-3.4 [16] is used to implement the constraints from  $B \rightarrow X_s \gamma$ . HiggsBounds-4.1.3 [17] is employed to implement the exclusion constraints from the neutral and charged Higgses searches at the LEP, Tevatron and LHC at 95% confidence level. Now we introduce the calculations of some constraints, which are the main motivations of this paper:

**Muon g-2:** The recent measurement on the muon anomalous magnetic moment is  $a_\mu^{exp} = (116592091 \pm 63) \times 10^{-11}$  [18], which has approximately  $3.1\sigma$  deviation from the SM prediction [19, 20],  $\Delta a_\mu = a_\mu^{exp} - a_\mu^{SM} = (262 \pm 85) \times 10^{-11}$  [9].

In the L2HDM,  $a_\mu$  gets the additional contributions from the one-loop diagrams induced by the Higgs bosons and also from the two-loop Barr-Zee diagrams mediated by  $A$ ,  $h$  and  $H$ . For the one-loop contributions [21],

$$\Delta a_\mu^{2\text{HDM}}(\text{1loop}) = \frac{G_F m_\mu^2}{4\pi^2 \sqrt{2}} \sum_j (y_\mu^j)^2 r_\mu^j f_j(r_\mu^j), \tag{8}$$

where  $j = h, H, A, H^\pm$ ,  $r_\mu^j = m_\mu^2/M_j^2$ . For  $r_\mu^j \ll 1$ ,

$$f_{h,H}(r) \simeq -\ln r - 7/6, \quad f_A(r) \simeq \ln r + 11/6, \quad f_{H^\pm}(r) \simeq -1/6. \tag{9}$$

For two-loop contributions,

$$\Delta a_\mu^{\text{2HDM}}(\text{2loop} - \text{BZ}) = \frac{G_F m_\mu^2}{4\pi^2 \sqrt{2}} \frac{\alpha_{\text{em}}}{\pi} \sum_{i,f} N_f^c Q_f^2 y_\mu^i y_f^i r_f^i g_i(r_f^i), \quad (10)$$

where  $i = h, H, A$ .  $m_f$ ,  $Q_f$  and  $N_f^c$  are the mass, electric charge and number of color degrees of freedom of the fermion  $f$  in the loop. The functions  $g_i(r)$  are [6, 7]

$$g_{h,H}(r) = \int_0^1 dx \frac{2x(1-x) - 1}{x(1-x) - r} \ln \frac{x(1-x)}{r}, \quad g_A(r) = \int_0^1 dx \frac{1}{x(1-x) - r} \ln \frac{x(1-x)}{r}. \quad (11)$$

The contributions of the CP-even (CP-odd) Higgses to  $a_\mu$  are negative (positive) at the two-loop level and positive (negative) at one-loop level. As  $m_f^2/m_\mu^2$  could easily overcome the loop suppression factor  $\alpha/\pi$ , the two-loop contributions may be larger than one-loop ones. In the L2HDM, since the CP-odd Higgs coupling to the tau lepton is proportional to  $\tan \beta$ , the L2HDM can enhance sizably the muon  $g-2$  for a light CP-odd Higgs with a large  $\tan \beta$ .

**Global fit to the 125.5 GeV Higgs signal data:** We take the light CP-even Higgs as the 125.5 GeV Higgs. Using the method taken in [22], we perform a global fit to the 125.5 GeV Higgs data of 29 channels after ICHEP 2014, which are summarized in the Tables I-V of [23]. A number of new measurements or updates of existing ones were presented by ATLAS and CMS Collaborations [3, 4, 24–31]. The signal strength for the  $i$  channel is defined as

$$\mu_i = \epsilon_{ggH}^i R_{ggH} + \epsilon_{VBF}^i R_{VBF} + \epsilon_{VH}^i R_{VH} + \epsilon_{t\bar{t}H}^i R_{t\bar{t}H}. \quad (12)$$

Where  $R_j = \frac{(\sigma \times BR)_j}{(\sigma \times BR)_j^{\text{SM}}}$  with  $j$  denoting the partonic processes  $ggH$ ,  $VBF$ ,  $VH$ , and  $t\bar{t}H$ .  $\epsilon_j^i$  denotes the assumed signal composition of the partonic process  $j$ , which are given in Tables I-V of [23]. For an uncorrelated observable  $i$ ,

$$\chi_i^2 = \frac{(\mu_i - \mu_i^{\text{exp}})^2}{\sigma_i^2}, \quad (13)$$

where  $\mu_i^{\text{exp}}$  and  $\sigma_i$  denote the experimental central value and uncertainty for the  $i$  channel. We retain the uncertainty asymmetry in our calculations. For the two correlated observables, we take

$$\chi_{i,j}^2 = \frac{1}{1 - \rho^2} \left[ \frac{(\mu_i - \mu_i^{\text{exp}})^2}{\sigma_i^2} + \frac{(\mu_j - \mu_j^{\text{exp}})^2}{\sigma_j^2} - 2\rho \frac{(\mu_i - \mu_i^{\text{exp}})(\mu_j - \mu_j^{\text{exp}})}{\sigma_i \sigma_j} \right], \quad (14)$$

where  $\rho$  is the correlation coefficient. We sum over  $\chi^2$  of the 29 channels, and pay particular attention to the surviving samples with  $\chi^2 - \chi_{\text{min}}^2 \leq 6.18$ , where  $\chi_{\text{min}}^2$  denotes the minimum of

$\chi^2$ . These samples correspond to the 95.4% confidence level regions in any two dimensional plane of the model parameters when explaining the Higgs data (corresponding to be within  $2\sigma$  range).

$B_s \rightarrow \mu^+ \mu^-$ : The LHCb [32] and CMS [33] measurements lead to the weighted average,  $\bar{B}(B_s \rightarrow \mu^+ \mu^-)_{exp} = (2.9 \pm 0.7) \times 10^{-9}$  [34], which is well agreement with the latest SM prediction,  $\bar{B}(B_s \rightarrow \mu^+ \mu^-)_{SM} = (3.65 \pm 0.23) \times 10^{-9}$  [35]. Recently, Ref. [36] presents a complete one-loop calculation of the contributions of Aligned 2HDM to  $B_s \rightarrow \mu^+ \mu^-$ . Following the method taken in Ref. [36], we define

$$\bar{R}_{s\mu} \equiv \frac{\bar{B}(B_s \rightarrow \mu^+ \mu^-)}{\bar{B}(B_s \rightarrow \mu^+ \mu^-)_{SM}} = \left[ |P|^2 + \left(1 - \frac{\Delta\Gamma_s}{\Gamma_L^s}\right) |S|^2 \right], \quad (15)$$

where the CKM matrix elements and hadronic factors cancel out. Combining the SM prediction with the experimental result,  $\bar{R}_{s\mu} = 0.79 \pm 0.2$  is required.

$$P \equiv \frac{C_{10}}{C_{10}^{SM}} + \frac{M_{B_s}^2}{2M_W^2} \left( \frac{m_b}{m_b + m_s} \right) \frac{C_P - C_P^{SM}}{C_{10}^{SM}}, \quad (16)$$

$$S \equiv \sqrt{1 - \frac{4m_\mu^2}{M_{B_s}^2}} \frac{M_{B_s}^2}{2M_W^2} \left( \frac{m_b}{m_b + m_s} \right) \frac{C_S - C_S^{SM}}{C_{10}^{SM}}. \quad (17)$$

The 2HDM can give the additional contributions to coefficient  $C_{10}$  by the  $Z$ -penguin diagrams with the charged Higgs loop. Unless there are large enhancements for  $C_P$  and  $C_S$ , their contributions can be neglected due to the suppression of the factor  $M_{B_s}^2/M_W^2$ . For example, the  $C_P$  and  $C_S$  of type-II 2HDM can be dominant due to the enhancement of the large  $\tan^2 \beta$  terms [37]. Although such large  $\tan^2 \beta$  terms are absent in the L2HDM,  $C_P$  can obtain the important contributions from the CP-odd Higgs exchange diagrams for  $m_A$  is very small. Such contributions are also sensitive to  $m_{H^\pm}$  and small  $\tan \beta$ . For the large  $\tan \beta$ , the terms proportional to  $\cot \beta$  and the higher order terms can be neglected.

Using the formulas in [36], we calculate the parameter  $P$  and  $S$  in the L2HDM. Note that the mixing of two CP-even Higgses in this paper is different from [36], therefore some corresponding couplings need be replaced.

In our calculations,  $m_h = 125.5$  GeV is fixed, and the input parameters are  $\sin(\beta - \alpha)$ ,  $\tan \beta$ , the physical Higgs masses ( $m_H, m_A, m_{H^\pm}$ ) and the coupling of  $hAA$  ( $\lambda_{hAA}$ ), where  $\lambda_{hAA}$  is used to replace the soft-breaking parameter  $m_{12}^2$ . We focus on  $5 \text{ GeV} < m_A < 62.75$  GeV, and such light CP-odd Higgs will be more strongly constrained, especially for the 125.5 GeV Higgs signal. Assuming that the Higgs couplings to fermions and gauge bosons are the

same as the SM,  $Br(h \rightarrow AA)$  is larger than 40% for  $|\lambda_{hAA}| > 20$  GeV and  $m_A < 62.5$  GeV. Therefore, we scan  $\lambda_{hAA}$  in the range of  $-20$  GeV  $\sim$   $20$  GeV. In addition to that the theoretical constraints are satisfied, we require the L2HDM to explain the experimental data within the  $2\sigma$  range, and fit the current Higgs signal data at the  $2\sigma$  level. The experimental values of electroweak precision data,  $B \rightarrow X_s \gamma$ ,  $\Delta m_{B_s}$  and  $\Delta m_{B_d}$  are taken from [38].

#### IV. RESULTS AND DISCUSSIONS

Without the constraint of muon g-2, we find a surviving sample with a minimal value of  $\chi^2$  fit to the Higgs signal data,  $\chi^2_{min} \simeq 16.95$ , which is slightly smaller than SM value, 17.0. The corresponding input parameters are,

$$\begin{aligned} \sin(\beta - \alpha) &\simeq -0.999994, \quad \tan \beta \simeq 5.16, \quad m_h = 125.5 \text{ GeV}, \quad m_H \simeq 130.35 \text{ GeV}, \\ m_A &= 61.50 \text{ GeV}, \quad m_{H^\pm} = 146.21 \text{ GeV}, \\ \lambda_{hAA} &\simeq -0.47 \text{ GeV} \quad (m_{12}^2 = 2174.84 \text{ GeV}^2). \end{aligned} \tag{18}$$

Our numerical results show that for the surviving samples within the  $2\sigma$  range of  $\chi^2$ ,  $Br(h \rightarrow AA)$  is required to be smaller than 24%. Considering the constraint of muon g-2, the minimal value is  $\chi^2_{min} \simeq 17.21$  and the input parameters are

$$\begin{aligned} \sin(\beta - \alpha) &\simeq 0.999712, \quad \tan \beta \simeq 84.90, \quad m_h = 125.5 \text{ GeV}, \quad m_H \simeq 504.34 \text{ GeV}, \\ m_A &= 57.00 \text{ GeV}, \quad m_{H^\pm} = 509.18 \text{ GeV}, \\ \lambda_{hAA} &\simeq -0.95 \text{ GeV} \quad (m_{12}^2 = 2995.28 \text{ GeV}^2). \end{aligned} \tag{19}$$

In Fig. 1, we project the surviving samples on the plane of  $\sin(\beta - \alpha)$  versus  $\tan \beta$ . Without the constraint of muon g-2, the surviving samples lie in two different regions. In one region, the 125.5 GeV Higgs couplings are near the SM values, called the SM-like region. In the other region, the Higgs couplings to leptons have opposite sign to the corresponding couplings to  $VV$ , called the wrong-sign Yukawa coupling region. In the SM-like region, the absolute value of  $\sin(\beta - \alpha)$  is required to be larger than 0.986, while  $\sin(\beta - \alpha)$  is allowed to have more sizable deviation from 1.0 in the wrong-sign Yukawa coupling region,  $\sin(\beta - \alpha) > 0.89$ . This can be understandable from the Higgs couplings to leptons. For the wrong-sign Yukawa coupling and SM-like Yukawa coupling, the Higgs couplings to lepton

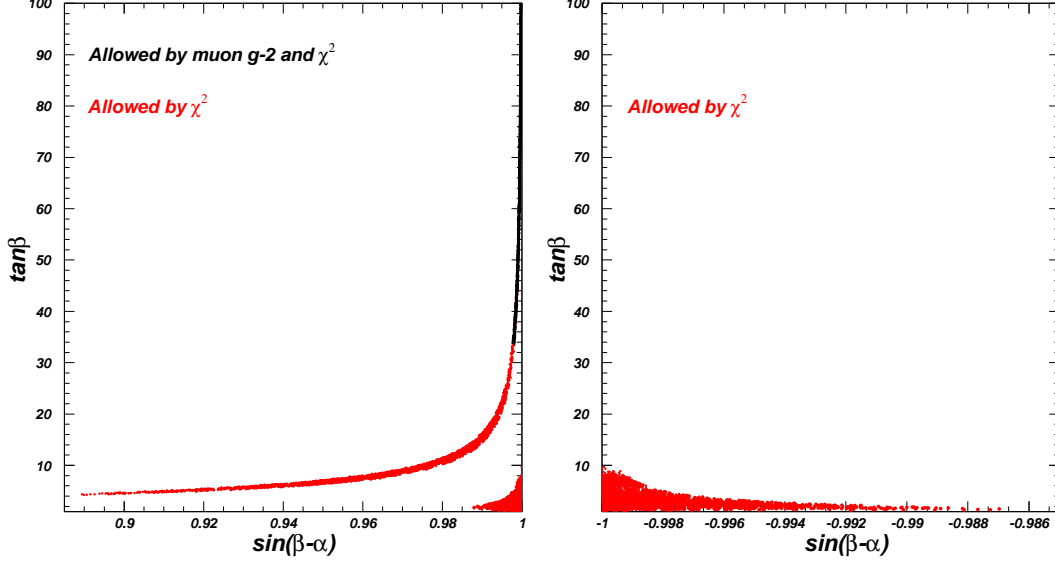


FIG. 1: The scatter plots of surviving samples projected on the plane of  $\sin(\beta - \alpha)$  versus  $\tan \beta$ .

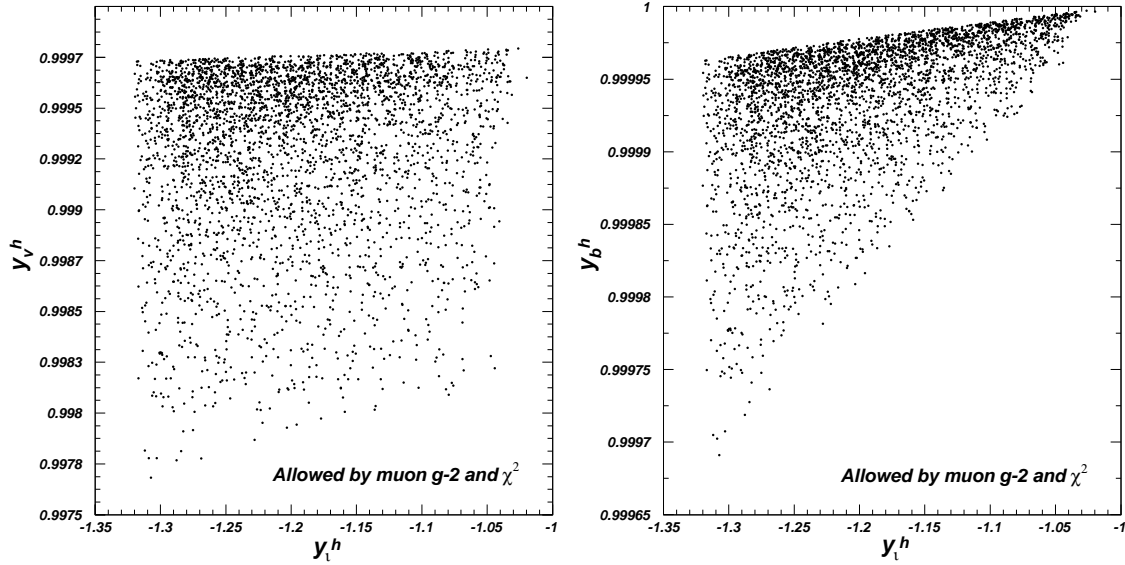


FIG. 2: The scatter plots of surviving samples with the  $2\sigma$  ranges of muon g-2 and  $\chi^2$  projected on the planes of the coupling  $h\ell\bar{\ell}$  versus  $hVV$ , and  $h\ell\bar{\ell}$  versus  $hb\bar{b}$ , respectively.

are respectively

$$\sin(\beta - \alpha) - \tan \beta \cos(\beta - \alpha) = -1 + \varepsilon, \quad \sin(\beta - \alpha) - \tan \beta \cos(\beta - \alpha) = 1 - \varepsilon, \quad (20)$$

where the absolute value of  $\varepsilon$  is much smaller than 1.0. For  $\sin(\beta - \alpha)$  approaches to 1.0,  $\cos(\beta - \alpha)$  of the former is much larger than that of the latter for the same  $\tan \beta$ .

Including the constraint of muon g-2, the surviving samples favor the wrong-sign Yukawa coupling region. The corresponding  $\sin(\beta - \alpha)$  approaches to 1.0 as increasing of  $\tan \beta$ ,



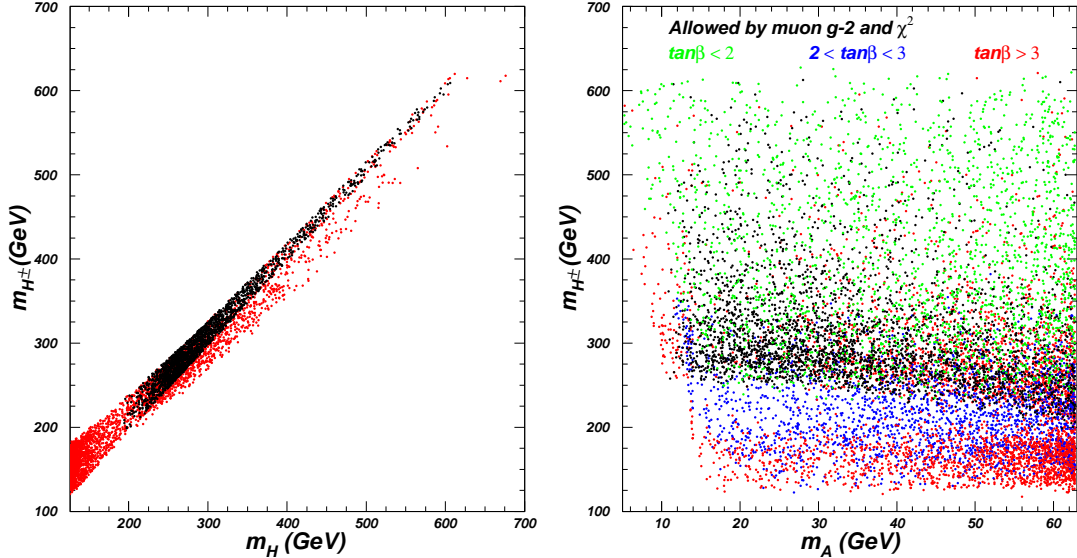


FIG. 3: Left panel: Same as Fig. 1, but projected on the plane of  $m_H$  versus  $m_{H^\pm}$ . Right panel: The scatter plots of surviving samples within the  $2\sigma$  range of  $\chi^2$  projected on the plane of  $m_A$  versus  $m_{H^\pm}$ .

leading a small  $\cos(\beta - \alpha)$  which ensures the absolute value of the coupling  $h\ell\bar{\ell}$  around SM value. To account for the muon  $g-2$ , L2HDM has to provide a very large pseudoscalar coupling to lepton, and  $\tan\beta$  is required to be larger than 34 as shown in the left panel of Fig. 1. For such large  $\tan\beta$ , Eq. (20) shows that  $y_\ell^h$  is much smaller than  $-1.0$  for  $\sin(\beta - \alpha)$  approaches to  $-1.0$ . As a result, the absolute value of the 125.5 GeV Higgs couplings to leptons have the sizable deviations from SM predictions, which is excluded by the  $2\sigma$  range of  $\chi^2$ . In addition, according to Eq. (20), such large  $\tan\beta$  leads to  $y_\ell^h < 0$  although  $\sin(\beta - \alpha)$  approaches to  $1.0$ . Therefore, the surviving samples lie in the wrong-sign Yukawa coupling region.

In Fig. 2, the surviving samples are projected on the planes of Higgs couplings. The Higgs couplings to  $VV$  and quarks are very closed to SM values, but the Higgs couplings to leptons have the opposite sign to the SM values, and over 30% deviation from the SM values.

In Fig. 3, the surviving samples are projected on the planes of  $m_H$  versus  $m_{H^\pm}$  and  $m_A$  versus  $m_{H^\pm}$ , respectively. The left panel shows that there is a small mass difference between  $m_H$  and  $m_{H^\pm}$  for the surviving samples, especially for including the constraint of muon  $g-2$ . Such small mass difference is mainly required by the electroweak parameter  $\rho$  to produce

a pseudoscalar with mass in the range of 5 GeV  $\sim$  62.75 GeV. As shown in Fig. 1, the experimental data of muon g-2 require  $\tan\beta > 34$ . For such large  $\tan\beta$ , the charged Higgs has a very large coupling to lepton, and the search experiments of charged Higgs give the lower bound of the charged Higgs mass,  $m_{H^\pm} > 200$  GeV. Due to the small mass difference between  $m_H$  and  $m_{H^\pm}$  induced by the parameter  $\rho$ ,  $m_H$  is required to be larger than 200 GeV. In Ref. [9], the authors took the limiting case of  $\beta - \alpha = \frac{\pi}{2}$  and several fixed values of  $m_H - m_{H^\pm}$  and  $\lambda_1$ , and found that the theoretical constraints and electroweak precision data give the upper bound of charged Higgs,  $m_{H^\pm} \leq 200$  GeV for  $m_A < 100$  GeV. In this paper, we scan the whole parameter space, and find that  $m_{H^\pm}$  is allowed to be as high as 600 GeV. Our results are consistent with those of many other papers, such as Ref. [39], Ref. [40] and Ref. [8].

The right panel shows that  $\tan\beta$  is required to be larger than 2.0 for  $m_{H^\pm} < 230$  GeV, and the main constraints are from the flavor observables  $\Delta m_{B_s}$  and  $\Delta m_{B_d}$ . In addition, for  $m_A < 16$  GeV, there is strong correlation between  $m_A$  and  $m_{H^\pm}$  due to the constraint of  $B_s \rightarrow \mu^+\mu^-$ . In particular,  $m_{H^\pm}$  is required to be larger than 450 GeV for  $\tan\beta < 2$  and  $m_A < 10$  GeV, and  $m_{H^\pm}$  is allowed to be sharply decreased with the increasing of  $m_A$ . For  $m_A > 20$  GeV, the contributions from the exchange of  $A$  diagrams to the coefficient  $C_P$  are difficult to overcome the suppression factor  $M_{B_s}^2/M_W^2$ , therefore  $B_s \rightarrow \mu^+\mu^-$  is not sensitive to  $m_A$ . Also the constraint of  $B_s \rightarrow \mu^+\mu^-$  on  $m_A$  and  $m_{H^\pm}$  can be relaxed by a modest large  $\tan\beta$ , but not sensitive to the enough large  $\tan\beta$ . Including the constraint of muon g-2,  $m_A$  is allowed to be as low as 10 GeV, but the corresponding  $m_{H^\pm}$  is required to be larger than 250 GeV.

In Fig. 4, the surviving samples are projected on the plane of  $m_A$  versus  $\tan\beta$ . For  $m_A < 26$  GeV, the upper bound of  $\tan\beta$  is strongly constrained by the exclusion experiments of Higgs at the collider, and some intermediate values are excluded by the  $2\sigma$  constraint of  $\chi^2$  fit to the Higgs signal. Including the constraint of muon g-2, the range of  $\tan\beta$  is sizably narrowed with  $m_A$  approaching to 10 GeV.

## V. CONCLUSION

In the L2HDM, a light pseudoscalar with a large  $\tan\beta$  can account for the muon g-2 anomaly. Assuming that the light CP-even Higgs is the 125.5 GeV Higgs, we study the

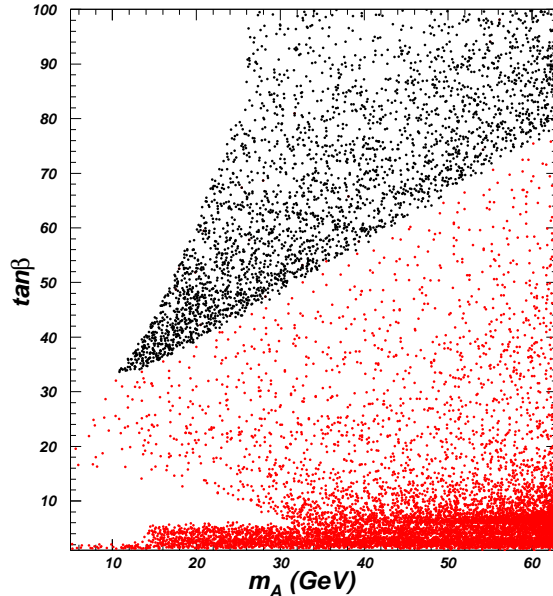


FIG. 4: Same as Fig. 1, but projected on the plane of  $m_A$  versus  $\tan\beta$ .

implications of the relevant theoretical and experimental constraints on a pseudoscalar with the mass below the half of 125.5 GeV, especially for the muon  $g-2$  anomaly, 125.5 GeV Higgs signal and  $B_s \rightarrow \mu^+\mu^-$ . We find that the pseudoscalar can be allowed to be as low as 10 GeV, and  $\tan\beta$  is required to be larger than 34. As the increasing of  $\tan\beta$ ,  $\sin(\beta - \alpha)$  is very closed to 1.0. For  $m_A$  approaches to 10 GeV, the range of  $\tan\beta$  is sizably narrowed, and  $m_{H^\pm}$  is required to be larger than 250 GeV. In addition, the 125.5 GeV Higgs couplings to leptons are favored to have opposite sign to the couplings to gauge bosons and quarks, and over 30% deviation from the SM values.

### Acknowledgment

We would like to thank Xin-Qiang Li for helpful discussions. This work was supported by the National Natural Science Foundation of China (NNSFC) under grant No. 11105116.

- 
- [1] S. Chatrchyan et al. [CMS Collaboration], Phys. Lett. B **716**, 30 (2012).
  - [2] G. Aad et al. [ATLAS Collaboration], Phys. Lett. B **716**, 1 (2012).
  - [3] G. Aad et al. [ATLAS Collaboration], arXiv:1408.7084.
  - [4] V. Khachatryan et al. [CMS Collaboration], Eur. Phys. Jour. C **74**, 3076 (2014).

- [5] see some recent examples: J. Bernon, J. F. Gunion, Y. Jiang, S. Kraml, arXiv:1412.3385; B. Dumont, J. F. Gunion, Y. Jiang, S. Kraml, Phys. Rev. D **90**, 035021 (2014); P. M. Ferreira, R. Guedes, M. O. P. Sampaio, R. Santos, JHEP **1412**, 067 (2014); P. S. B. Dev, A. Pilaftsis, JHEP **1412**, 024 (2014); L. Wang, X.-F. Han, JHEP **1411**, (2014) 085; Phys. Lett. B **739**, 416 (2014); B. Grzadkowski, O. M. Ogreid, P. Osland, JHEP **1411**, 084 (2014); S. Kanemura, K. Tsumura, K. Yagyu, H. Yokoya, Phys. Rev. D **90**, 075001 (2014); A. Kobakhidze, L. Wu, J. Yue, JHEP **1410**, 100 (2014); B. Hespel, D. Lopez-Val, E. Vryonidou, JHEP **1409**, 124 (2014); J. Baglio, O. Eberhardt, U. Nierste, M. Wiebusch, Phys. Rev. D **90**, 015008 (2014); K. Cheung, J. S. Lee, P.-Y. Tseng, JHEP **1401**, 085 (2014); P. M. Ferreira, R. Santos, J. F. Gunion, H. E. Haber, Phys. Rev. D **89**, 115003 (2014); B. Coleppa, F. Kling, S. Su, JHEP **1401**, 161 (2014); X.-D. Cheng, Y.-D. Yang, X.-B. Yuan, Eur. Phys. Jour. C **74**, 3081 (2014); Y.-N. Mao, S.-H. Zhu, arXiv:1409.6844; N. Chen, J. Li, Y. Liu, Z. Liu, arXiv:1410.4447; A. Celis, V. Ilisie, A. Pich, JHEP **1312**, 095 (2013); C.-Y. Chen and S. Dawson, Phys. Rev. D **87**, 055016 (2013); V. Barger, L. L. Everett, H. E. Logan and G. Shaughnessy, Phys. Rev. D **88**, 115003 (2013); X.-F. Wang, C. Du, H.-J. He, Phys. Lett. B **723**, 314 (2013); T. Abe, N. Chen, H.-J. He, JHEP **1301**, 082 (2013); J. Shu, Y. Zhang, Phys. Rev. Lett. **111**, 091801 (2013).
- [6] D. Chang, W.-F. Chang, C.-H. Chou, and W.-Y. Keung, Phys. Rev. D **63**, 091301 (2001); K. Cheung, C.-H. Chou, and O. C. Kong, Phys. Rev. D **64**, 111301 (2001).
- [7] K. Cheung, O. C. Kong, Phys. Rev. D **68**, 053003 (2003).
- [8] J. Cao, P. Wan, L. Wu, J. M. Yang, Phys. Rev. D **80**, 071701 (2009).
- [9] A. Broggio, E. J. Chun, M. Passera, K. M. Patel, S. K. Vempati, JHEP **1411**, 058 (2014).
- [10] L. J. Hall, M. B. Wise, Nucl. Phys. B **187**, 397 (1981); J. F. Donoghue, L. F. Li, Phys. Rev. D **19**, 945 (1979).
- [11] V. D. Barger, J. L. Hewett, R. J. N. Phillips, Phys. Rev. D **41**, 3421 (1990); Y. Grossman, Nucl. Phys. B **426**, 3 (1994); A. G. Akeroyd, W. J. Stirling, Nucl. Phys. B **447**, 3 (1995); A. G. Akeroyd, Phys. Lett. B **377**, 95 (1996); A. G. Akeroyd, J. Phys. G **24**, 1983 (1998); M. Aoki, S. Kanemura, K. Tsumura, K. Yagyu, Phys. Rev. D **80**, 015017 (2009).
- [12] R. A. Battye, G. D. Brawn, A. Pilaftsis, JHEP **1108**, 020 (2011).
- [13] S. Davidson, H. E. Haber, Phys. Rev. D **72**, 035004 (2005), Erratum-ibid. D **72**, 099902 (2005).

- [14] A. Pich, P. Tuzon, Phys. Rev. D **80**, 091702 (2009).
- [15] D. Eriksson, J. Rathsmann, O. Stål, Comput. Phys. Commun. **181**, 189-205 (2010); Comput. Phys. Commun. **181**, 833-834 (2010).
- [16] F. Mahmoudi, Comput. Phys. Commun. **180**, 1579-1673 (2009).
- [17] P. Bechtle, O. Brein, S. Heinemeyer, G. Weiglein, K. E. Williams, Comput. Phys. Commun. **181**, 138-167 (2010); P. Bechtle, O. Brein, S. Heinemeyer, O. Stål, T. Stefaniak, G. Weiglein, K. E. Williams, Eur. Phys. Jour. C **74**, 2693 (2014).
- [18] G. Bennett et al. [Muon G-2 Collaboration Collaboration], Phys. Rev. D **73**, 072003 (2006).
- [19] F. Jegerlehner, A. Nyffeler, Phys. Rept. **477**, 1-110 (2009).
- [20] A. Kurz, T. Liu, P. Marquard, M. Steinhauser, Phys. Lett. B **734**, 144-147 (2014).
- [21] B. Lautrup, A. Peterman, E. de Rafael, Phys. Rept. **3**, 193-260 (1972); J. P. Leveille, Nucl. Phys. B **137**, 63 (1978); A. Dedes, H. E. Haber, JHEP **0105**, 006 (2001).
- [22] J. R. Espinosa, C. Grojean, M. Muhlleitner, M. Trott, JHEP **1205**, 097 (2012); G. Belanger, B. Dumont, U. Ellwanger, J. F. Gunion, S. Kraml, JHEP **1302**, 053 (2013); P. P. Giardino, K. Kannike, M. Raidal, A. Strumia, JHEP **1206**, 117 (2012); B. Dumont, S. Fichet, G. Gersdorff, JHEP **1307**, 065 (2013); J.-J. Cao, Z.-X. Heng, J. M. Yang, Y.-M. Zhang, J.-Y. Zhu, JHEP **1203**, 086 (2012); J. S. Lee, P. Y. Tseng, JHEP **1305**, 134 (2013).
- [23] K. Cheung, J. S. Lee, P.-Y. Tseng, Phys. Rev. D **90**, 095009 (2014).
- [24] G. Aad et al. [ATLAS Collaboration], Phys. Rev. D **90**, 052004 (2014).
- [25] Talk by C. Mills, "Measurement of Cross Sections and Couplings of the Higgs Boson in the WW decay Channel using the ATLAS detector", ICHEP 2014, Spain.
- [26] Talk by E. Shabalina, "Search for Higgs Bosons produced in association with top quarks with the ATLAS detector", ICHEP 2014, Spain.
- [27] Plenary talk by M. Kado, "Physics of the Brout-Englert-Higgs boson in ATLAS", ICHEP 2014, Spain.
- [28] S. Chatrchyan et al. [CMS Collaboration], Phys. Rev. D **89**, 092007 (2014); JHEP **1401**, 096 (2014); Phys. Rev. D **89**, 012003 (2014); JHEP **1405**, 104 (2014).
- [29] The CMS Collaboration, "Search for ttH events in the  $H \rightarrow b\bar{b}$  final state using the Matrix Element Method", CMS-PAS-HIG-14-010.
- [30] Plenary talk by A. David, "Physics of the Brout-Englert-Higgs boson in CMS", ICHEP 2014, Spain.

- [31] Talk by K. Herner, "Studies of the Higgs boson properties at D0", ICHEP 2014, Spain.
- [32] R. Aaij et al. [LHCb Collaboration], Phys. Rev. Lett. **111**, 101805 (2013).
- [33] S. Chatrchyan et al. [CMS Collaboration], Phys. Rev. Lett. **111**, 101804 (2013).
- [34] CMS and LHCb Collaborations, CMS-PAS-BPH-13-007.
- [35] C. Bobeth, M. Gorbahn, T. Hermann, M. Misiak, E. Stamou, M. Steinhauser, Phys. Rev. Lett. **112**, 101801 (2014).
- [36] X.-Q. Li, J. Lu, A. Pich, JHEP **1406**, 022 (2014).
- [37] H. E. Logan, U. Nierste, Nucl. Phys. B **586**, 39-55 (2000); C.-S. Huang, W. Liao, Q.-S. Yan, Phys. Rev. D **59**, 011701 (1999).
- [38] K. A. Olive et al. [Particle Data Group], Chin. Phys. C **38**, 090001 (2014).
- [39] B. Dumont, J. F. Gunion, Y. Jiang, S. Kraml, Phys. Rev. D **90**, 035021 (2014).
- [40] B. Coleppa, F. Kling, S. Su, JHEP **1401**, 161 (2014).